PHYSICAL REVIEW B VOLUME 18, NUMBER 1 1 JULY 1978

Quadrupolar nuclear resonance in electron-irradiated aluminum: Electric field gradients around vacancies and interstitials

M. Minier and R. Andreani
Laboratoire de Spectrométrie Physique, Université Scientifique et Médicale de Grenoble Boite Postale 53, 38041 Grenoble Cedex, France*

C. Minier
Département de Recherche Fondamentale, Section de Physique du Solide Centre d'Etudes Nucléaires de Grenoble, 85 X, 38041 Grenoble Cedex, France

(Received 18 November 1977)

Nuclear quadrupolar couplings around defects created by electron irradiation in aluminum have been measured by the nuclear-magnetic-resonance field-cycling technique. The wipe-out numbers are roughly estimated to be 300 ± 100 and 1000 ± 200 for the monovacancy and self-interstitial, respectively. The electric-field-gradient values on the four first atomic shells around a monovacancy have been determined and are compared with quadrupolar couplings around impurities in aluminum. The asymmetry parameter η at the first neighbors of the monovacancy is rather large ($\eta = 0.65$). Using existing theory, it is shown that this value must be associated with a strong relaxation around the monovacancy. The experimental results rule out the possibility of a spherical symmetry around the self-interstitial, in agreement with other experimental observations. The quadrupolar couplings measured after the different stages of annealing of defects after irradiation are well explained with a model in which free interstitials migrate in stage I, small clusters rearrange themselves in stage II, and monovacancies migrate in stage III.

I. INTRODUCTION

Point defects created in metals by irradiation or quenching have been studied for many years by various techniques but little information is available about the associated electronic perturbation. Recently, many calculations based on the electron theory of metals or on the effective interionic potential theory have tried to predict the physical properties of vacancies and interstitials. Thus, it is important to check the validity of the interatomic potentials used by comparison of the results of these calculations with experimental data from the most direct technique available. Nuclear magnetic resonance (NMR), which can measure the electric-field-gradient (EFG) values associated with the screening charge, is a good technique for such a test of validity.

Moreover, in the case of vacancy-type defects, the physical properties observed by different methods are generally associated with monovacancies, divacancies, and larger clusters. Consequently, it is often difficult to analyze the contribution of each defect type. We will demonstrate that a specific NMR technique allows the characterization of monovacancies independently of other vacancy-type defects.

The classical NMR technique is able to measure the range of the perturbation created by the defect, while a specific technique which has been used here (the so-called field-cycling technique) measures the values of the EFG at the nuclei of the different shells around the defect, leading to a more detailed knowledge of the electronic perturbation.[1] Several impurities have been studied in aluminum[2,3] and the purpose of this experiment was to extend these measurements to the EFG around vacancies in aluminum. The preparation of a sample suitable for NMR experiments and which contains a large enough concentration of monovacancies ($\sim 0.01\%$) presents serious difficulties if quenching techniques are used. Thus, the creation of this defect by electron irradiation was chosen; self-interstitials are created simultaneously and the interpretation of the spectra takes into account both types of defects.

The experiments that are presented here give the values of the EFG for the four nearest-neighbor shells of a monovacancy and give information about the range of the perturbation created by vacancies and interstitials in aluminum. The relaxation of the nearest neighbors of the vacancy is also discussed.

II. EXPERIMENTAL TECHNIQUES AND PROCEDURES

A. Experimental devices

An NMR probe containing the sample is placed inside a liquid-hydrogen irradiation cryostat connected to a cryogenerator. It is bombarded with electron accelerated to an energy of 3 MeV by a Van de Graaff machine; then it is carefully transferred without any heating to the NMR cryostat containing liquid helium. The sample is made of 30 99.999% pure aluminum foils 60 μm thick pre-

annealed for 2 h at 250 °C. The foils are electrically insulated from each other by a resinous coating which remains unaltered by electron irradiation.

The resonance coil is a 200-μm-thick copper wire wound around the foils without contact and held in place with the same resin. An aluminum wire 200 μm in diameter is wound around the central foil to monitor resistivity, and hence the effects of the irradiation and thermal annealing. Energy losses at the center of the sample due to the absorption of the different components were calculated to be only 0.3 MeV; furthermore, the sample is rotated through 180° halfway through the irradiation. Under these conditions, the resistivity increase of the central aluminum wire during irradiation gives a reasonably good measure of the defect concentration in the whole sample. The coil containing the sample is supported by a brass holder in which a copper-constantan thermocouple and a carbon resistor are fixed to allow temperature measurement and control. At the end of the irradiation the sample is raised into a shielded reservoir filled with liquid hydrogen and transferred into the NMR cryostat containing liquid helium. Then it is pushed down into the center of the superconducting coil which provides the magnetic field. The subsequent thermal treatments are performed by raising the sample into the gas above the liquid helium.

B. Point-defect creation in aluminum by electron bombardment

Irradiation of aluminum with 3-MeV electrons at 20 K creates an equal number of metastable vacancies and self-interstitials. This increases the resistivity of the sample by an amount ΔR_0. Some interstitials are created in the vicinity of their own vacancy and together they form so-called close Frenkel pairs . Furthermore, some isolated interstitials are formed and these do not interact strongly with their own vacancies.

During warm-up of a sample irradiated at low temperature the interstitials migrate in the crystal and are annihilated when they meet a vacancy; a strong decrease in resistivity is associated with this mechanism. Other interstitials combine to form di-interstitials and larger clusters but the associated resistivity variation is much smaller.

In aluminum,[4] the first resistivity decrease after a 20-K irradiation is called stage IC and is centered around 30 K; it is attributed to the annihilation of close pairs of a given configuration. The structure of this close pair is not well established but in nickel it has been proposed[5] that the stage analogous to IC is due to Frenkel pairs where the interstitial is centered on the fifth-nearest neighbor of the vacancy. Between 30 and 50 K the stages ID and IE, which together account for 40% to 50% of ΔR_0, are attributed to the annihilation of interstitials which are not in interaction with their own vacancy. At temperatures higher than 50 K, only vacancies and interstitial clusters remain. Stage II occurs between 50 and 150 K and increases in importance with initial defect concentration; this complex stage is often associated with a reorganization of interstitial clusters and partial annihilation by the vacancies. During stage III, between 150 and 300 K, the resistivity recovers its preirradiation value. This corresponds to the disappearance of all the remaining defects created by the irradiation.

C. NMR field-cycling technique

A detailed analysis of this technique and a description of the apparatus are given in Refs. 6–8. It is sufficient to note that the rf absorption of nuclear spins in zero external magnetic field is detected. Thus, an absorption between 0 and 30 kHz is always observed with a maximum at around 10 kHz. It is due to the nuclei subjected to the dipolar interaction of their neighbors. If they exist, nuclei which experience quadrupolar couplings larger than the dipolar one also give rise to several lines at higher frequency.

In the case of a dilute substitutional alloy, a plot of the number of aluminum nuclei as a function of the EFG value to which they are subjected gives rise to several peaks corresponding to the various shells of nuclei around the impurity, as a consequence of the spherical symmetry. Each of the EFG gives rise to two quadrupolar transitions in case of aluminum ($\pm\frac{1}{2}\rightarrow\pm\frac{3}{2}$ and $\pm\frac{3}{2}\rightarrow\pm\frac{5}{2}$) which in the example illustrated in Fig. 1 will be well defined for the first shells and hidden by the dipolar absorption at lower frequencies for higher-order shells. The detection of these quadrupolar transitions by the field-cycling technique depends on an exchange of energy with the dipolar reservoir of nuclei subjected to dipolar interactions only. Below 160 kHz, cross relaxation is usually good in aluminum and irradiation in zero field is carried out with one rf field and called the single-irradiation (SI) technique. Above this frequency a more sophisticated method with two rf fields is used and referred to as the double-irradiation (DI) technique.

The intensity of the observed quadrupolar lines depends on the number of nuclei involved; this in turn helps with the identification of the different shells around the defect. The intensity also depends on the cross-relaxation process with the dipolar reservoir and of the technique used for

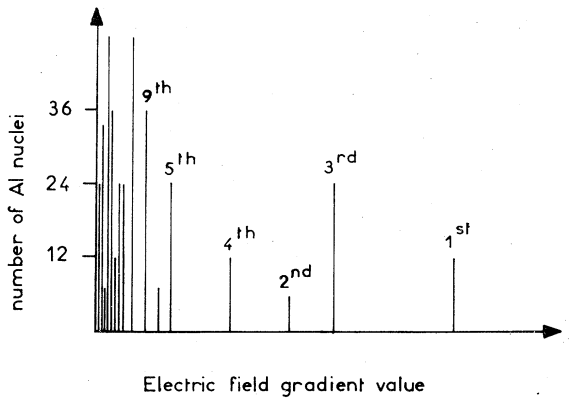

FIG. 1. Number of aluminum nuclei as a function of the EFG value to which they might by subjected. Only some of the closest shells are numbered. Generally, the EFG to which a given neighbor shell is subjected depends upon the alloy and the position of the first. shell could be, for example, at a smaller EFG than the third shell.

their detection (SI technique or DI technique). Furthermore, couplings between near-neighbor spins give rise to solid-effect quadrupolar lines, which are rather easily identified and which are helpful in the classification of the quadrupolar transitions.

From the frequencies ν of the two quadrupolar transitions $\pm\frac{1}{2}\rightarrow\pm\frac{3}{2}$ and $\pm\frac{3}{2}\rightarrow\pm\frac{5}{2}$, the value of the EFG can be deduced, as well as its asymmetry parameter η which is a measure of a nonaxial symmetry[9]

$$\eta=(V_{yy}-V_{xx})/V_{zz},$$

where V_{xx}, V_{yy}, and V_{zz} are the principal values of the EFG tensor, with $V_{xx}\leq V_{yy}\leq V_{zz}$ (usually we shall write $V_{zz}=eq$).

η can vary from 0 for cylindrical symmetry about the z axis, to 1, and consequently the ratio $\nu_{3/2\rightarrow 5/2}/\nu_{1/2\rightarrow 3/2}$ varies from 2 to 1.

In the case of a defect with noncubic symmetry, a plot of the number of aluminum nuclei as a function of the EFG value experienced does not show well-defined peaks, since the q values are spread out; the corresponding quadrupolar transitions overlap to produce a continuous absorption. Then the spin energy of each transition can easily cross relax with the dipolar reservoir. Consequently, the SI technique will detect this continuous absorption.

D. Experimental procedure

Before irradiation, the absorption spectrum of the sample in zero field is recorded at 1.4 K, as well as the initial resistivity of the aluminum wire. After irradiation, the spectrum shows additional absorption due to quadrupolar couplings around the defects. Subsequently the sample is heated to 30 K in order to annihilate the close Frenkel pairs, the effect of this annealing is checked by resistivity, and the new absorption spectrum recorded. The same procedure is repeated after heating to 50 K (after stage IE), to 150 K (after stage II) and finally 300 K (after stage III).

III. EXPERIMENTAL RESULTS

A. Characterization of the sample before irradiation

The zero-field absorption spectrum (Fig. 2) shows only a dipolar absorption. The spin-lattice relaxation time T_1, at 1.4 K, is 560 msec in zero field and 1200 msec in 500 G. The ratio confirms that the sample contains only a few imperfections[10] which cannot be detected by NMR. The resistivity of the monitoring wire is 2.4×10^{-9} Ω cm at 4 K and 4.5×10^{-9} Ω cm at 20 K.

B. Electron irradiation

Tests of the increase of the resistivity as a function of the irradiation current show that an intensity of 15 μA increases the temperature of the sample by only a few degrees. This intensity was maintained for about 100 h. The sample was rotated through 180° after 50 h to ensure a better homogeneity of the concentration of defects created in the foils.

The resistivity measured after irradiation was 89×10^{-9} Ω cm at 20 K. After the transfer to liquid helium, the resistivity was 86×10^{-9} Ω cm, which proved that no significant heating of the sample occurred during the transfer.

C. Quadrupolar spectra

1. Spectrum after irradiation

As shown in Fig. 3, the defects created by irradiation considerably modify the absorption in zero field measured by the SI technique. The sharp dipolar absorption of Fig. 2 has become in a broad one, up to 160 kHz, and extends to even more than 350 kHz with lower intensity. This absorption is due to a continuous distribution of quadrupolar transitions. The closeness of these transitions allows an easy diffusion of spin energy toward the dipolar reservoir and increases considerably its "capacity."[3] A rather intense and broad absorption appears at 300 kHz, and weaker absorptions are also detected between 350 and 480 kHz, and between 600 and 800 kHz.

A search for other lines has been carried out using the DI technique up to 2 MHz but without

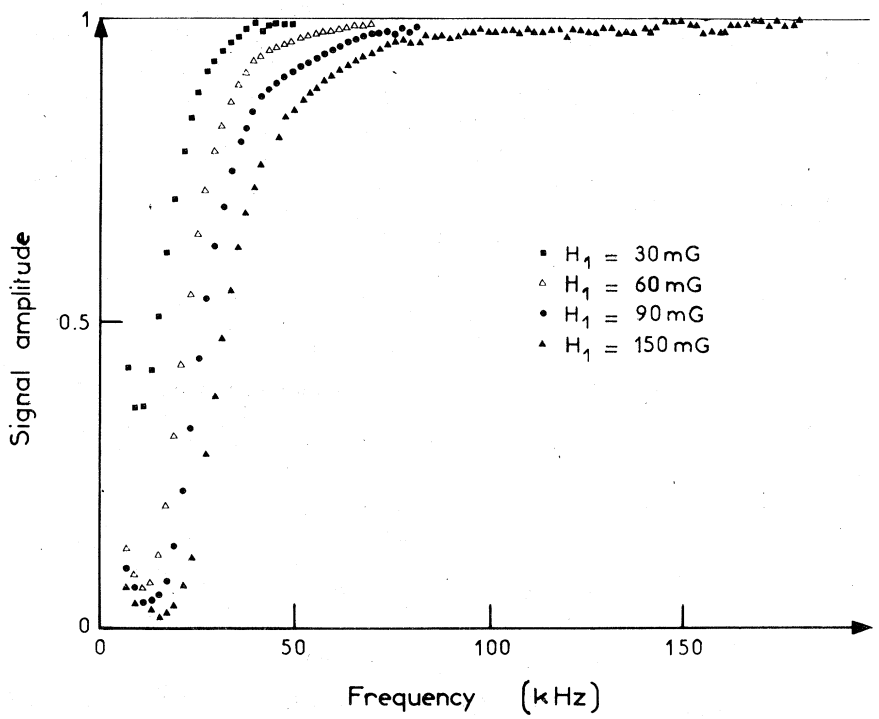

FIG. 2. Zero-field absorption spectrum of the aluminum sample before irradiation.

success. Even if such lines exist, they could hardly be detected; the small amount of energy transferred by this method to the dipolar spin reservoir, compared with the large heat capacity of this reservoir after irradiation, leads to a small increase of the spin temperature and thus to a very weak line in the spectrum. T_1 at 1.4 K is 400 msec in zero field and 1200 msec in high field. Their ratio of about 3 confirms the existence of strong quadrupolar interactions in zero field.

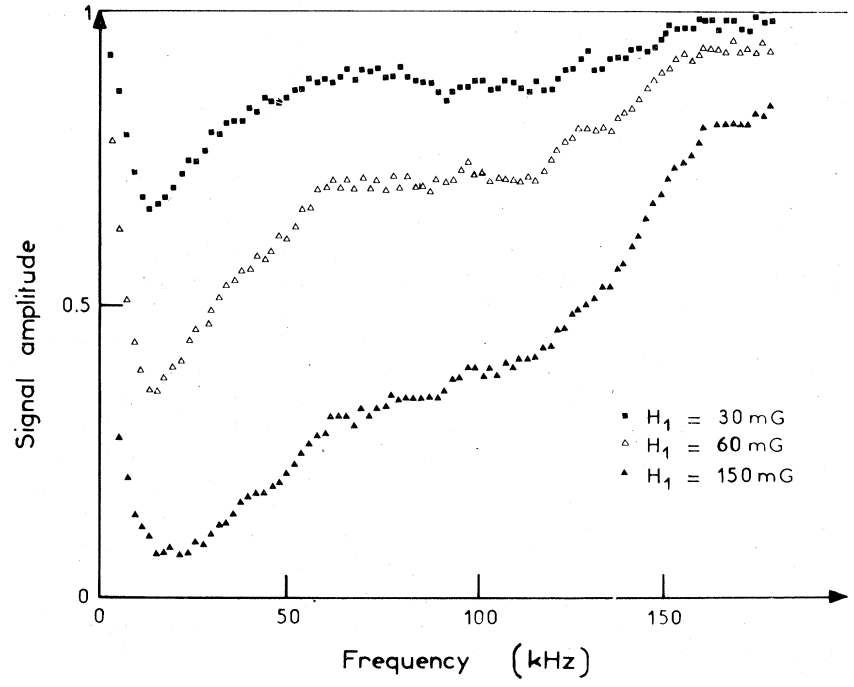

FIG. 3. Low-frequency part of the single-irradiation recordings in the aluminum sample just after irradiation.

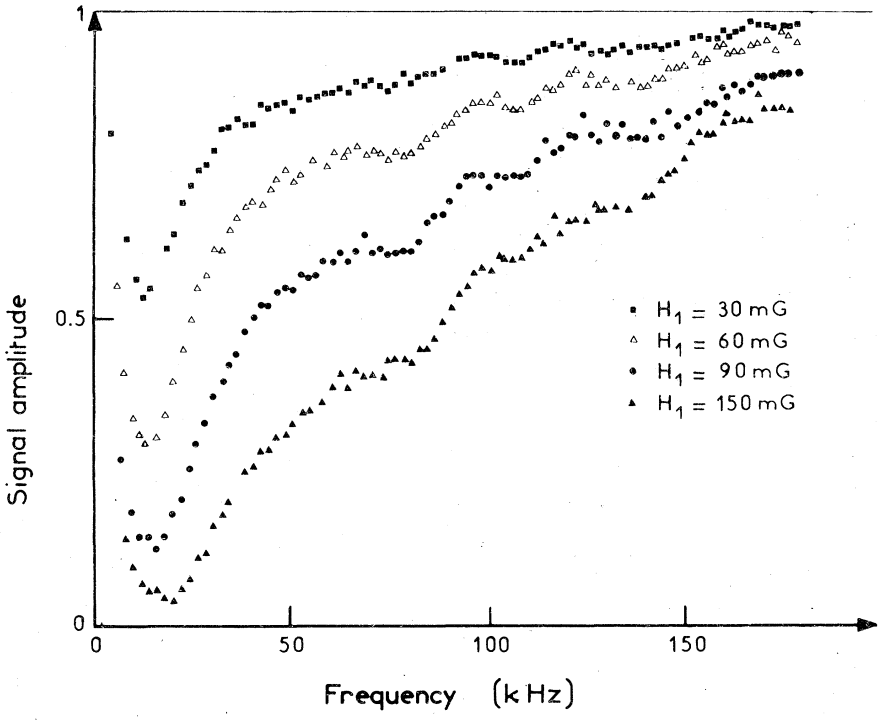

FIG. 4. Low-frequency part of the single-irradiation recordings in the aluminum sample after annealing at 50 K.

2. First annealing at 30 K

In order to anneal out the stage IC, the sample is heated at 30 K for 15 min. The residual resistivity does not change, and the quadrupolar spectrum remains unmodified. It is probable that this temperature has been reached during irradiation, and this stage already annealed out.

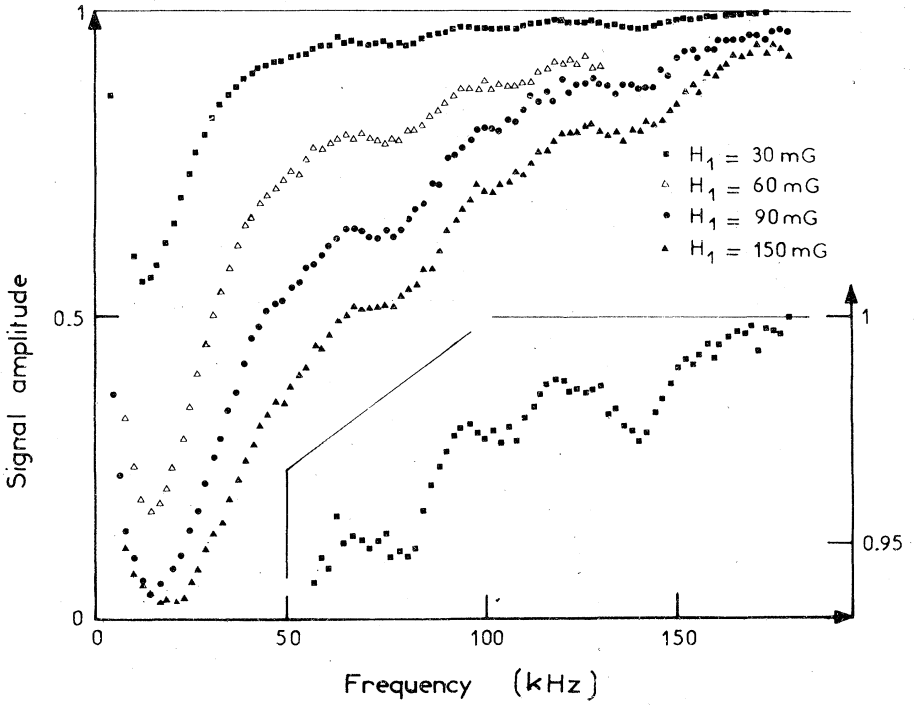

FIG. 5. Low-frequency part of the single-irradiation recordings in the aluminum sample after annealing at 150 K.

3. Annealing at 50 K

The sample is then heated for 25 min at 50 K, in order to anneal the stages I*D* and I*E*. The residual resistivity measured at 4 K becomes $\rho = 55 \times 10^{-9}$ Ω cm. Several modifications of the quadrupolar spectrum observed after irradiation can be seen:

(a) The continuous absorption is considerably reduced (Fig. 4) and the dipolar absorption is increased; this means that many nuclei which experienced quadrupolar couplings larger than dipolar couplings are now subject only to weak quadrupolar perturbations.

(b) Slightly more intense absorptions appear around 50, 70, 100, and 140 kHz. They could be due to quadrupolar transitions of nuclei situated on shells around a specific defect.

(c) The lines in the SI spectrum at 300 kHz and around 400 kHz have completely disappeared together with the absorption between 600 and 800 kHz.

(d) The DI technique allows the observation of two weak but well defined lines at 300 and 400 kHz.

4. Annealing at 150 K

In order to anneal out stage II, the sample is heated to 150 K for 30 min. The residual resistivity decreases to 34×10^{-9} Ω cm. The continuous absorption is again reduced, leading to a more accurate recording of the lines at 50 ± 5, 75 ± 3, 105 ± 3, and 140 ± 3 kHz using the SI technique (Fig. 5) and at 305 ± 5 and 405 ± 5 kHz using the DI technique (Fig. 6). The decrease in the continuous absorption also permits the observation of a weak and rather broad absorption around 215 kHz, when high rf fields are used. Search for other lines has been carried out up to 2 MHz (the highest frequency for a $\frac{1}{2} \rightarrow \frac{3}{2}$ transition in an aluminum alloy has been found[3] in *Al*Ti, at 674 kHz).[3]

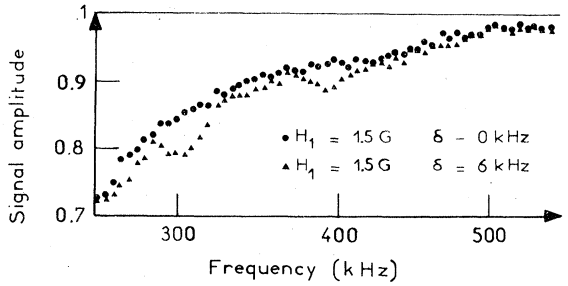

FIG. 6. Double-frequency-irradiation recordings of the aluminum sample between 250 and 550 kHz after annealing at 150 K. δ is the frequency separation between the two rf fields. When $\delta = 0$, double-irradiation technique is equivalent to the single-irraditation technique.

5. Annealing at room temperature

After 3 h at 300 K, the resistivity at 4 K is the same as before irradiation (2.4×10^{-9} Ω cm) and the quadrupolar spectrum is identical to that recorded before irradiation (Fig. 2).

IV. INTERPRETATION

It is useful to estimate the concentrations of vacancies and interstitials at different stages of the experiment. Choosing a value of 4×10^{-4} Ω cm per unit concentration of Frenkel pair[11] one obtains 0.021% of such pairs after irradiation, 0.013% after annealing at 50 K, and 0.008% after annealing at 150 K. Only 40% of Frenkel defects disappear at stage I, when 60% to 70% should have disappeared for such an irradiation at 20 K. This observation confirms that the stage I*C* has been annealed during irradiation. Since the same resistivity and identical quadrupolar spectra are obtained before irradiation and after the annealing at 300 K, all the modifications observed at the various stages of the experiment must be assigned to defects created by irradiation and annealed out by the thermal treatments.

A. Quadrupolar spectrum after stage II

Since after annealing at 150 K, the defect population consists mainly of interstitial clusters and isolated vacancies, the well-resolved quadrupolar lines obtained must be assigned to monovacancies. Their intensities are consistent with a concentration of the order of 0.008%. The quadrupolar spectrum is very similar to that obtained for several impurities in aluminum[2] and the identification of the lines is rather easy.

No pure-quadrupolar transitions are observed between 150 and 300 kHz and above 405 kHz. Consequently, the two lines at 305 and 405 kHz are identified as the $\pm \frac{1}{2} \rightarrow \pm \frac{3}{2}$ and $\pm \frac{3}{2} \rightarrow \pm \frac{5}{2}$ transitions of nuclei in the same shell. Since their frequencies are much higher than those of the other transitions, give a high-asymmetry parameter η, and are similar to those observed in aluminum alloys, they are assigned to the 12 nuclei in the nearest-neighbor shell of the vacancy; this leads for these sites to

$$q_1 = 2.8 \times 10^{23}\ \text{cm}^{-3}, \quad \eta_1 = 0.65.$$

The absorption at 215 kHz presents all the characteristics of a "quadrupolar solid effect" transition[7] associated with the two lines at 75 and 140 kHz which are paired off. Because of the intensities of these two lines and of the 215-kHz absorption they are assigned to the 24 nuclei in the third-nearest-neighbor shell of the vacancy, for

which $\pm\frac{1}{2}\rightarrow\pm\frac{5}{2}$ transition probability is large in the solid effect. Thus, we have

$$q_3 = 9.3\times 10^{22}\ \text{cm}^{-3}.$$

The two transitions at 105 kHz and around 50 kHz are assigned to the 12 fourth-nearest neighbors by a comparison of their intensities with those of the corresponding transitions of the third neighbors. This leads to

$$q_4 = 6.9\times 10^{22}\ \text{cm}^{-3}.$$

The six second-neighboring nuclei are not detected, either because the intensity of the lines is too weak or because their transitions are situated below 50 kHz. There are two very weak absorptions near 65 and 125 kHz which could be assigned to the second-neighbor shell, but the signal-to-noise ratio is of the order of one!

The wipe-out number[12] is a rough measure of the number of nuclei which experience EFG's greater than a critical value for which the quadrupolar splitting is of the order of the dipolar linewidth. Although the field-cycling technique is not the best one to determine these wipe-out numbers, it gives a rough estimate. It is clear that the nuclei which give well-resolved quadrupolar lines are included in the wipe-out number, but nuclei experiencing quadrupolar couplings only slightly larger than the dipolar value also participate. These nuclei increase the dipolar absorption on the high-frequency side, particularly since there are more of them. It results, for example, in the fact that the number of well-resolved quadrupolar lines, and the shape of the dipolar absorption are completely different for *Al*Mn (wipe out: 1600) than for *Al*Zn (wipe out: 90).

In irradiated aluminum, comparing the quadrupolar spectra obtained after stage II to those for several aluminum alloys for which wipe-out numbers have been measured, it is possible to estimate a wipe-out number of 300 ± 100 for the monovacancy. The comparison also clearly shows that a weak continuous-absorption extending up to 400 or 500 kHz is superimposed on the quadrupolar lines due to the monovacancies, we have attributed it to the nuclei around the clusters of interstitial atoms; although clusters are not numerous, the perturbation around them is probably very strong and the quadrupolar couplings perturb a large number of nuclei. We shall see how this is confirmed by the spectrum obtained just after irradiation.

B. Quadrupolar spectrum after irradiation

The concentration of vacancies is now approximately 0.02%, or three times the concentration after annealing at 150 K. Interstitials are present at the same concentration, but they are isolated from each other, and not in the form of clusters as was the case after stage II.

The main difference compared with the spectrum obtained after stage II is the strong continuous absorption and a relative decrease of the dipolar absorption. These modifications are not due to the vacancies because, as mentioned above, they give rise to well-defined quadrupolar lines while causing a moderate decrease in the dipolar intensity. Thus, they must be attributed to the existence of interstitials. It is not surprising that these interstitials do not give rise to well defined lines, as it is usually accepted that they are in a dissociated form. Such dissociated defects lead to a continuous absorption (see Sec. II C).

Furthermore, the large modification of the dipolar absorption with such a small concentration of defects is noteworthy. By comparing the general form of the spectrum to those for aluminum alloys containing a similar concentration of impurities, one can estimate the wipe out number of the interstitial to be approximately 1000 ± 300.

The second main difference from the spectrum obtained after stage II is the detection of the broad absorption at 300 kHz, between 350 and 480 kHz, and between 600 and 800 kHz. Although our arguments are not conclusive, an explanation in agreement with experimental observation can be advanced: the line at 300 kHz is always associated with the $\pm\frac{1}{2}\rightarrow\pm\frac{3}{2}$ transition of the nearest neighbors of the vacancy. However, any interstitial nuclei close to the vacancy create quadrupolar couplings of the same order of magnitude. Consequently, the energy absorbed by the nuclei near vacancies can cross relax to the dipolar reservoir with the help of the continuous distribution of quadrupolar couplings around interstitials. Also, the perturbation around interstitials broadens the quadrupolar transition at 300 kHz and this explains why the corresponding $\pm\frac{3}{2}\rightarrow\pm\frac{5}{2}$ which was at 405 kHz when the monovacancies were isolated now appears as a broad absorption between 350 and 480 kHz. The weak absorption between 600 and 800 kHz can probably be attributed to various quadrupolar solid effect transitions.

C. Quadrupolar spectrum after stage I

The recovery of the dipolar absorption, and the decrease in the continuous absorption which makes the quadrupolar transition around vacancies more apparent form the main features of the spectrum compared to the measurements just after irradiation. Qualitatively, these modifications cannot be explained by a decrease in the interstitial con-

centration from 0.021% to 0.013%, unless one now considers interstitials to have precipitated to form complexes such as di-interstitials.

Second, the lines at 305 and 405 kHz are observed by the DI technique, and present a normal width. This fact is a consequence of the annealing of close Frenkel defects: the vacancies are now at large distances from the interstitial complexes. The nuclei around them are not perturbed, and cannot transfer their energy to the dipolar reservoir, the nuclei which could transfer the energy are now too far away.

V. DISCUSSION

A. EFG values at large distance from the defect: Wipe-out number

The wipe-out number is mainly sensitive to EFG values at large distances from the defect. These EFG values are proportional to the screening charge which is given in the framework of a simple model[13] by

$$\Delta\rho \sim \sum_l (2l+1)(-1)^l \sin\eta_l \frac{\cos(2k_F r + \eta_l)}{r^3},$$

where η_l are the phase shifts describing the scattering, while the impurity resistivity is

$$\Delta R \sim \sum_l l \sin^2(\eta_{l-1} - \eta_l).$$

These two quantities have their origin in the scattering of the electrons by the perturbing potential of the defect and they both increase with it.

Since the EFG is proportional to $\Delta\rho(r)$, the wipe-out number must have the same behavior as ΔR. Resistivities and wipe-out numbers for alloys with different impurities are given in Table I. For the vacancy, the latest results for the resistivity lie between 1 and 1.5 $\mu\Omega$ cm/at.%.[14,15] It has been shown that the resistivity of an interstitial is roughly twice that of the vacancy,[16] the value 2–3 $\mu\Omega$ cm/at.% is consistent with the resistivity of a Frenkel pair of the order of 4 $\mu\Omega$ cm/at.%.[11] A similar variation of the wipe-out numbers and the resistivity data is apparent in Table I.

In fact, the EFG are proportional to $\Delta\rho(r)$ only to a first approximation: another contribution due to a size effect which pushes the nuclei from their original sites and breaks the cubic symmetry must be considered. In the elastic approximation this contribution to the EFG is proportional to the fractional change in the lattice parameter $(1/a)(da/dc)$, with a coefficient λ which relates the experimental EFG to the EFG which would be observed if the distorted lattice were made up of unshielded point charges.[17] This contribution decreases as r^{-3}, or the same way as the charge effect. In aluminum alloys, a relationship between the wipe-out number and $(1/a)(da/dc)$ is not obvious and it is difficult to deduce any information on the relaxation around the vacancies from the wipe-out number.

B. EFG values on the nearest shells around a defect

Theoretical prediction of the exact values of the EFG at the nearest shells around the perturbing potential is much more difficult than that of the wipe-out numbers or resistivity, which are dependent on a value of the potential averaged over the various crystallographic directions. Calculations performed in aluminum using pseudopotential theory give a good value for resistivities[18] or even for wipe-out numbers but are unable to predict the values of the EFG on the first shells.[19,20] It would probably be necessary to go beyond the spherical approximation to take into account the nonsphericity of the Fermi surface and to consider carefully all the possible contributions to EFG at the nearest-neighbor shells.

Experimentally, one can point out that a mono-

TABLE I. Residual resistivity values and wipe-out number values of monovacancy, interstitial, and several impurities in aluminum.

	Vacancy	Interstitial	Zn	Mg	Si	Cu	Cr	Mn
ΔR ($\mu\Omega$ cm/at.%)	from 1 to 1.5	from 2 to 3	0.3[a]	0.5[a]	0.8[a]	0.8[a]	7[b]	7[b]
Wipe-Out number	300 ±100	1000 ±200	94[c]	122[c]	199[c]	236[c]	1620[d]	1380[d]

[a] G. Revel, Mem. Sci. Rev. Metall. 65, 181 (1968).

[b] E. Babic, R. Krsnik, B. Leontić, M. Očko, Z. Vučić, and E. Girt, Solid State Commun. 10, 691 (1972).

[c] Y. Fukai *et al.*, Ref. 19.

[d] G. Grüner, E. Kovacs-Csetenyi, K. Tompa, and C. R. Vassel, Phys. Status Solidi 45, 663 (1971).

TABLE II. Values of the fractional change in lattice parameter and of the asymmetry parameter of the EFG on the nearest neighbors in several aluminum alloys.

	Mg	Si	Cu	Zn	Ga	Ge	Ag	Cd	In	Sc	Ti	V	Cr	Mn	Fe	Vacancy
$\frac{1}{a}\frac{da}{dc}$	0.099[a]	−0.042[a]	−0.092[a]	−0.013[a]	0.045[a]	0.045[a]	0.023[a]	−0.09[a]	0[a]	0.12[b]	−0.12[b]	−0.13[b]	−0.17[b]	−0.18[b]	−0.13[b]	
η	0.07[c]	0.03[c]	0.23[c]	0.27[c]	0.03[c]	0.03[c]	0.31[c]	0.03[c]	0.30[c]	0.05[d]	0.06[d]	0.12[d]	0.23[d]	0.32[d]	0.57[d]	0.65

[a] W. B. Pearson, *Handbook of Lattice Spacings and Structure of Metals and Alloys* (Pergamon, New York, 1958).
[b] M. Očko, E. Babic, and V. Zlatic, Solid State Commun. 18, 705 (1976).
[c] M. Minier *et al.*, Ref. 2.
[d] C. Berthier *et al.*, Ref. 3.

vacancy creates EFG's on the neighboring shells similar to those created around normal impurities, except for the high value of the asymmetry parameter η on the first shell (see Table II). The origin of this asymmetry deserves a special discussion because, in principle, it can give information about the relaxation around a monovacancy.

First of all, as in the case of impurities,[2,3,21-24] it should be noted that η is clearly different from zero only for the first-neighbor shell, suggesting that a particular effect takes place for these nuclei. Recently, Sagalyn and Alexander[25] have interpreted the η values on the nearest neighbors of impurities in several copper alloys by combining a charge effect, which leads to $\eta = 0$, with a size effect. The latter, treated in a point-charge model, completely modifies the symmetry of the EFG tensor. To fit the experimental values of q and η at the first neighbors, they use an EFG strain coupling constant which leads to a size-effect contribution of the same order of magnitude as the charge effect. A similar analysis has been given by Süto[26] for aluminum containing $3d$ transition impurities.

If the size effect produces the η values, one can say that vacancy which leads to a η value of 0.65 has a much more important size effect than normal impurities which give η values less than 0.35 even though the $(1/a)(da/dc)$ values vary over a wide range (see Table II). This particularly strong size effect would hardly be consistent with a weak relaxation around vacancy. In fact, we can conclude that there is a particularly strong contraction of the nearest-neighbor shell for two reasons: (i) Only an expansion or contraction much larger than that which has ever been deduced for the case of impurities in metals could explain the high η value. Of these, an anomalous contraction seems to be more feasible. (ii) A series effect appears for η for $3d$ transition impurities. η increases regularly from scandium to iron (Table II) though the ionic radius of the impurity decreases. The negative $(1/a)(da/dc)$ values show an increasing bulk contraction (except for iron). Although charge effects are particularly strong in these instances, this behavior seems to indicate that η increases with increasing contraction.

The idea of a contraction is consistent with the result of Singhal.[27] The pair potential determined by Singhal for pure aluminum is repulsive at the first and second neighbors, implying that a given atom "pushes" its neighbors outwards. If this atom is removed, creating a vacancy, the neighbors will therefore move in towards the space vacated.

Our conclusion that there is an overall contraction around the vacancy in aluminum is based on

the size-effect contribution to the η value and on qualitative arguments which require a detailed theoretical analysis. Nevertheless, the η measurement is probably the only technique at the present time available which can, in principle, lead to an evaluation of the displacement of the nearest-neighbor nuclei around a vacancy.

Measurements of the formation volume of a vacancy take into account the relaxation of all the atoms around it and care must be taken in a comparison of these data with ours, which concern only the first shell. In the case of aluminum, the situation is not very clear at the moment: the formation volume has been experimentally found to be 0.65 (Ref. 28) or 0.55 (Ref. 29) atomic volume, indicating a contraction of the lattice. Other experiments[30] have given a value very close to 1.

VI. CONCLUSION

We have measured quadrupolar couplings related to the screening charge around monovacancies in aluminum. In particular, the values of the EFG determined on the four nearest-neighbor shells may be used as a test for the potentials proposed to calculate physical properties.

The value of the asymmetry parameter of the EFG on a vacancy nearest-neighbor shell is much higher than for impurities in aluminum. This can be related to an important relaxation of the nearest neighbors. We give arguments why the relaxation is negative, i.e., a contraction.

The NMR technique presented here is a new method to study defects created by irradiation and particularly to characterize the monovacancy independently of interstitials, divacancies, or clusters.

For the interstitial, the results exclude a site of lattice symmetry, such as an octahedral site, in agreement with existing theories. The high value of the estimated wipe-out number for the interstitial shows that it strongly perturbs the interatomic potential.

The results obtained at the different stages of annealing are compatible with a model where the free interstitial migrates during stage I, small clusters of interstitials are rearranged during stage II, and the monovacancy migrates during stage III.

ACKNOWLEDGMENTS

The authors wish to express their thanks to the Section des Accélérateurs and the Service des Basses Températures of the Centre d'Etudes Nucléaires de Grenoble for their technical assistance in carrying out the irradiations.

---

*Associated with the CNRS.
[1]G. Grüner and M. Minier, Adv. Phys. 26, 231 (1977).
[2]M. Minier and S. Hodung, J. Phys. F 7, 503 (1977).
[3]C. Berthier and M. Minier, J. Phys. F 7, 515 (1977).
[4]W. Schilling, G. Burger, K. Isebeck, and H. Wenzl, *Vacancies and Interstitials in Metals* (North-Holland, Amsterdam, 1970), p. 255.
[5]P. Peretto, J. L. Oddou, C. Minier-Cassayre, D. Dautreppe, and P. Moser, Phys. Status Solidi 16, 281 (1966).
[6]A. G. Redfield, Phys. Rev. 130, 589 (1963).
[7]C. Berthier, M. Minier, Phys. Rev. B 7, 1854 (1973).
[8]R. Andreani, thesis (Université de Grenoble, 1975) (unpublished).
[9]A. Abragam, *The Principles of Nuclear Magnetism* (Clarendon, Oxford, 1961).
[10]E. R. Andrew, W. S. Hinshaw, and R. S. Tiffen, J. Phys. F 4, L215 (1974).
[11]H. Wenzl, in Ref. 4, p. 363.
[12]N. Bloembergen and T. J. Rowland, Acta Metall. 1, 731 (1953).
[13]J. M. Ziman, *Principles of the Theory of Solids* (Cambridge U. P., Cambridge, England, 1964).
[14]K. Furukawa, J. Takamura, N. Kuwana, R. Tahara, and M. Abe, J. Phys. Soc. Jpn. 41, 1585 (1976).
[15]P. Tzanetakis, thesis (Université de Grenoble, 1977) (unpublished).
[16]C. Budin, R. Brugiere, and P. Lucasson, Mem. Sci. Rev. Metall. 64, 891 (1967).
[17]P. L. Sagalyn, A. Paskin, and R. J. Harrison, Phys. Rev. 124, 428 (1961).
[18]Y. Fukai, Philos. Mag. 20, 1277 (1969).
[19]Y. Fukai, and K. Watanabe, Phys. Rev. B 2, 2353 (1970).
[20]P. M. Holtham and P. Jena, J. Phys. F 5, 1649 (1975).
[21]L. Jorgensen, R. Nevald, and D. L. Williams, J. Phys. F 1, 972 (1971).
[22]L. E. Drain, Phys. Rev. B 8, 3628 (1973).
[23]R. Nevald, B. L. Jensen, and P. B. Fynbo, J. Phys. F 4, 1320 (1974).
[24]J. Stiles, N. Kaplan, and D. L. Williams, J. Phys. F 5, 1993 (1975).
[25]P. L. Sagalyn and M. N. Alexander, Phys. Rev. B 15, 5581 (1977).
[26]A. Süto (private communication).
[27]S. P. Singhal, Phys. Rev. B 8, 3641 (1973).
[28]R. M. Emrick and P. B. McArdle, Phys. Rev. 188, 1156 (1969).
[29]R. R. Bourassa, D. Lazarus, and D. A. Blackburn, Phys. Rev. 165, 853 (1968).
[30]E. A. Harrison and P. Wilkes, J. Phys. E 5, 174 (1972).